CHAPTER-3

Solution-processed, Highly-efficient Organic-Inorganic nano-composite Field-effect Transistor based Hydrogen Sulfide Gas Sensor at sub-ppm Regime

3.1 Introduction 69
3.2 Experimental section 71
3.2.1. Materials Used 71
3.2.2. Device Fabrication 71
3.2.3. Gas Sensing Setup 73
3.3 Thin film Morphology 74
3.4 Results and discussion 76
3.4.1. Electrical Characterization 76
3.5 Gas Sensing Parameters 78
3.5.1. Gas Sensing Response 78
3.5.2. Selectivity 78
3.5.3. Stability and Relative Humidity Influence Analysis 79
3.5.4. Repeatability and Transient Analysis 80
3.5.5. gas sensing mechanism 81
3.6 Conclusion 85

The part of the work is adopted from-

V. K. Singh and V. N. Mishra, "Solution Processed Highly Efficient H_2S Gas Sensor with Sub-ppm Detection Limit Based on Self-Aligned Thin Film of PCPDTBT Decorated with CdS Nanoparticles," in ***IEEE Transactions on Electron Devices***, vol. 70, no. 8, pp. 4351-4358, Aug. 2023, ***doi: 10.1109/TED.2023. 3287509..***

ABSTRACT

In previous chapter the developed sensor has demonstrated poor recovery characteristics, environmental degradation, significant reliance on relative humidity variation, less mobility, and a possibility to further enhance the sensing response. In regards to improve all these parameters, the nanocomposite of organic-inorganic material has been utilized. The synergistic effect between these two classes of materials helped in improving the stated parameters. Further, photoirradiation of composite solution has facilitated the molecular ordering of the polymer composite matrix, which further enhanced the charge transport properties of the sensing layer. In present work, a facile method to develop PCPDTBT/CdS composite thin film with the integration of photoirradiation of the nanocomposite solution, simple and inexpensive floating film transfer deposition method (FTM), and solvent vapor annealing (SVA) has been demonstrated. The film is applied to organic field-effect transistor (OFET) in top contact bottom gate (TCBG) configuration, to evaluate the gas sensing performance for various concentrations of reducing and toxic H_2S gas, at room temperature. Synergetic effect of the photoirradiation, presence of CdS, FTM, and SVA enhances the molecular ordering of the polymer matrix. Photoirradiated PCPDTBT/CdS nanocomposite film exhibits a maximum charge carrier mobility of ~$3.4*10^{-3}$ $cm^2/V.$ s, which is many folds higher than the pristine PCPDTBT film. Favourable π-π and electrostatic interactions after photoirradiation and self-aligned nature of FTM film enhances the interfacial interactions between CdS and PCPDTBT. Additionally, state-of-the-art technique 'solvent vapor annealing' offers enhanced crystallinity, excellent charge transport along the polymer chain which, significantly improves sensitivity. Photoirradiated-SVA annealed PCPDTBT/CdS composite film based OFET sensors consistently show enhanced sensitivity compared to the pristine PCPDTBT, and

PCPDTBT/CdS composite. Particularly, the photoirradiated-SVA annealed PCPDTBT/CdS composite sensor achieves significantly enhanced response of ~81% to 1 ppm exposure of H_2S gas, compared to the pristine PCPDTBT (~71%), and PCPDTBT/CdS (~76%) nanocomposites. Additionally, excellent response-recovery behaviour (e.g., ~5 s and ~ 90 s, respectively), good ambient stability, and excellent selectivity are also observed.

3.1 Introduction

To date, numerous organic polymer (Polyaniline, Polypyrrole, Polyphenylene, Polyacetylene, P3HT, PBTTT, PQT-12, etc.), semiconducting inorganic materials (metals, metal oxides, transition metal disulfides, monosulfides, etc.), and doping techniques have been used to enhance the film morphology and improve electrical conductivity and sensitivity in an effort to improve H_2S gas-sensing performance [84][85]. These organic and inorganic semiconductor-based hydrogen sulfide gas sensors have accomplished excellent research improvements in terms of good sensitivity, better selectivity, and quick response/recovery properties [51], [86]–[89]. Furthermore, organic materials have issues related to low conductivity, poor ambient stability, and strong affinity to volatile organic substances [90] and inorganic materials possess the limitations in terms of high-temperature operation, solid-substrate limit, poor selectivity, and complicated processability [91]. These limitations hinder their use in highly efficient gas sensor fabrication. Moreover, using a nanocomposite of an organic semiconducting polymer and an inorganic material to produce extremely effective gas sensors has drawn a lot of interest in gas-sensing applications because of their synergistic effects. These synergistic effects in organic-inorganic composite enable to eradicate their inherent flaws while also incorporating the merits of their organic and inorganic counterparts in gas-sensing applications, leading to the development of highly effective materials for gas sensors [92]. The synergistic

interactions between the inorganic and polymeric components act as dopants for the counterparts, demonstrating that the conductivity is dependent on these interactions. Cadmium sulphide (CdS) is a direct band gap II-VI compound inorganic semiconductor that has received a lot of attention in the photovoltaic field. Moreover, CdS has drawn interest from researchers due to its relative affordability, processability as thin films and nanocomposites (NCs), and potential use in a variety of fields, including photonics, photoconducting components, logic gates, field effect transistors, solar cells etc. Cadmium sulphide (CdS) has been also found sensitive to various toxic and hazardous gases due to its tailorable properties, tuneable surface morphology, and suitability for NCs formation. Therefore, we have utilized the PCPDTBT/CdS nanocomposite to investigate the electrical and Hydrogen sulfide gas sensing properties. A facile photoirradiation approach has been utilized to enhance the molecular ordering of the polymer chain in nanocomposite solution. After being exposed to UV light, the chains of PCPDTBT present in the composite solution underwent to photoexcited state, which results in enhanced π-π interactions, planarization of the PCPDTBT polymer chain, and subsequent delocalization of π-electrons throughout the backbone of the polymer. Through the numerous favourable nucleation sites for crystal growth, such as defects and vacancies, the planarized PCPDTBT chains started to adsorb on the CdS surface. Consecutively, enhanced π-π interactions at the nucleation sites results in the stacked PCPDTBT chains, which further results in crystalline growth of PCPDTBT. The improved interfacial interactions between CdS and PCPDTBT, as well as the enhanced charge transport characteristics, were obtained with the resulting PCPDTBT/CdS composite films [93]. Subsequently, polymer nanocomposite film has been deposited using the floating film transfer method (FTM), as illustrated in previous chapter [45]. After thin film deposition, in order to improve the π-π stacking of the polymer chain, crystallinity and charge transfer along the polymer backbone, we

further employed the solvent vapour annealing (SVA) technique as depicted in previous chapter [71][72]. We have utilized top contact bottom gate (TCBG) OFET due to its sensitive detection, multiparametric analysis capabilities, and inheriting a number of potential advantages. Therefore, to the best of our knowledge, possibly for the first time, all above mentioned points motivated us to fabricate a OFET sensor utilizing PCPDTBT/CdS nanocomposite as an active sensing layer and conduct extensive studies to investigate the electrical and gas sensing properties of PCPDTBT/CdS nanocomposite thin film to integrate all the advantages of the organic-inorganic nanocomposites as stated above.

3.2 Experimental section

3.2.1. Materials Used

Poly[2,6-(4,4-bis-(2-ethylhexyl)-4H-cyclopenta [2,1-b;3,4-b′] dithiophene)-alt-4,7(2,1,3-benzothiadiazole)] (PCPDTBT MW 7k – 20k) and powder form CdS nanoparticles (NPs) were procured from Sigma Aldrich Pvt. Ltd. and Ossila Ltd. respectively. Acetone, isopropyl Alcohol, toluene, ODTS (octadecyl trichlorosilane), chloroform, methanol, and any other chemical used was procured form Merck India Pvt. ltd. All the chemicals have been used without any further purification or process.

3.2.2. Device Fabrication

10 mg of pristine PCPDTBT polymer and 2 mg of CdS nanoparticles were dissolved/dispersed separately in 1 ml chloroform solution. The solutions were kept on constant stirring at 900 rpm for 1.5 hours at room temperature (RT-25 ºC). Further, both the solutions were mixed to form a 5 w/v % PCPDTBT/CdS nanocomposite solution. The nanocomposite solution was then agitated at 900 rpm for 60 minutes at RT to form a homogenous solution. Subsequently, the composite solution was photoirradiated (**Figure 3.1**(a)) by being subjected to UV light for 10 minutes while being gently stirred. Finally, we have

three solutions, PCPDTBT (S_1), PCPDTBT/CdS composite (S_2), and photoirradiated PCPDTBT/CdS composite (S_3). The architecture of the fabricated gas sensing device and enlarged device image as depicted in **Figure 3.1(b)** and **Figure 3.1(c),** is based on an organic semiconducting polymer composite operating as the active layer in a top-contact, bottom-gate OFET structure. The following procedure has been utilized for the fabrication of the Organic FET. A heavily doped p++ Silicon wafer is cleaned by the standard wet cleaning process. The dry oxidation of the cleaned wafer is carried out to grow 300 nm (measured by Filmetrics F20-UV) SiO_2 (Oxide) film to utilize as an oxide/dielectric layer. The grown oxide has an oxide capacitance of ~10 nF/cm^2. Further, the surface was treated with O_2 (oxygen) plasma for 5 minutes to obtain an activated surface with uniform surface energy. Further, to passivate the activated surface charge trapping sites and to obtain a hydrophobic surface (improves the semiconducting film adhesion), surface treatment of the Si/SiO_2 wafer was performed using octadecyl trichlorosilane solution (ODTS) (~5 nm monolayer). The thermally grown Si/SiO_2 was dipped for 12 hrs. in 1 mM ODTS solution in toluene, subsequently the substrate was washed with toluene several times and dried. A drop of the polymer/ composite solution (10 mg/ml in chloroform) was dispensed on an Eg: Gl (3:1) mixture (liquid substrate of hydrophilic nature). This combination of liquid substrate was selected since it has been observed that this concentration produces films with the highest anisotropy [74].

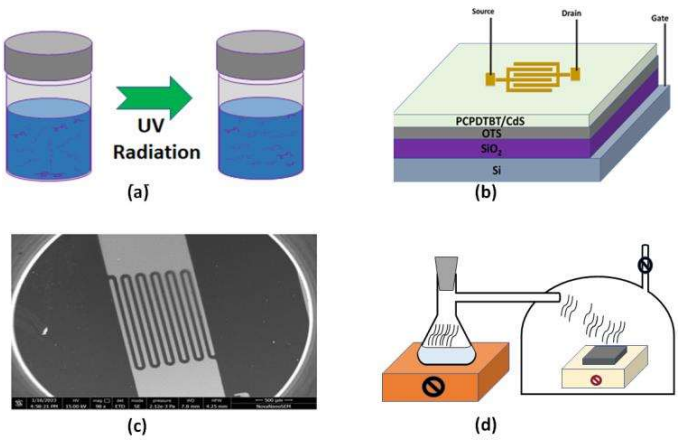

Figure 3.1 Schematic representation of the (a) Photoirradiation, (b) Device architecture, (c) Enlarged device image, and (d) Solvent vapor annealing, respectively.

Dynamic evaporation of the solvent (chloroform) over the liquid substrate developed a long floating thin film. The oriented region of this film was recognized using a polarizer sheet and stamped onto the ODTS-treated Si/SiO_2 substrate. In an Argon glove box, the samples were annealed at 70°C for 30 min. Further, we used Chlorobenzene (CB) vapor to anneal the film for 1 hr (solvent vapor annealing). The FTM deposited substrate was placed in a closed container which contains an inlet with an opening and closing valve. Another airtight container with chlorobenzene solvent was heated until it produced vapors at a nearly constant rate. Then with the help of an airtight pipe, vapors of chlorobenzene were passed to the inlet of the substrate container for 1 hr (**Figure 3.1(d)).** Afterward, thermally evaporated, 50 nm thickness gold (Au) drain and source electrodes were deposited by HHV 12A4D thermal coating unit at a constant pressure of $\sim 10^{-6}$ torr. Finally, we have obtained three devices named D_1 (pristine PCPDTBT), D_2 (PCPDTBT/CdS composite), and D_3 (photoirradiated PCPDTBT/CdS composite) from the solutions S_1, S_2, and S_3 respectively.

3.2.3. Gas Sensing Setup

The indigenous sensing setup developed in our lab has been used for the gas sensing

characterization. A mass flow controller (MFC) for controlling dilution and analyte gas concentration is included in the sensing setup chamber along with a probe contact, humidity sensor, mixing fan, sample/analyte gas (H_2S), dilution (or purging) gas (N_2 (79%) and O_2 (21%)), gas inlet valve, gas exhaust valve, and a temperature-controlled chuck. The semiconductor parameter analyzer KEYSIGHT B1500A unit has evaluated the characterization of the device's electrical and gas sensing properties. All of the sensing characterization in the current work has been performed at room temperature with a relative humidity of 55%.

3.3 Thin film Morphology

The **Figure 3.2** demonstrate the atomic force microscopic image of the nanocomposite polymer matrix (over the SiO2 /Si substrate) with and without the photoirradiation. The AFM characterization was done by the NT-MDT, Model - NTEGRA Prima in tapping mode. The **Table 3.1** demonstrates the extracted parameters of the sensing film morphology. We can observe that the grain size and length has been decreased significantly for the Photoirradiated PCPDTBT/CdS composite film, while the RMS roughness is higher compared to pristine PCPDTBT and PCPDTBT/CdS composite film. The grain analysis of the sensing film presented in **Figure 3.2(c), Figure 3.2(f),** and **Figure 3.2(i)** demonstrates that the Photoirradiated film has developed a large number of grain boundaries compared to pristine and PCPDTBT/CdS composite film due to decreased grain size. Furthermore, from **Figure 3.2**, we can observe that the photoirradiated film is slightly better aligned and offers better connected grains. As shown in **Figure 3.2(i),** the interconnected neighboring grains provide a better percolation path for the charge transfer along the active sensing film and enhance the charge transport process. The number of grain boundaries and surface roughness are crucial parameters for the enhanced gas adsorption (physisorption) process. Also, the aligned nature of the film and well-connected grains

are crucial for a better charge transport process. As described earlier, the parameters mentioned above have been improved significantly, thus improving the physisorption and charge transport process and enhancing sensitivity. All the improvements discussed in surface morphology are due to the combined effect of the photoirradiation of the composite solution, floating film transfer deposition, and solvent vapor annealing.

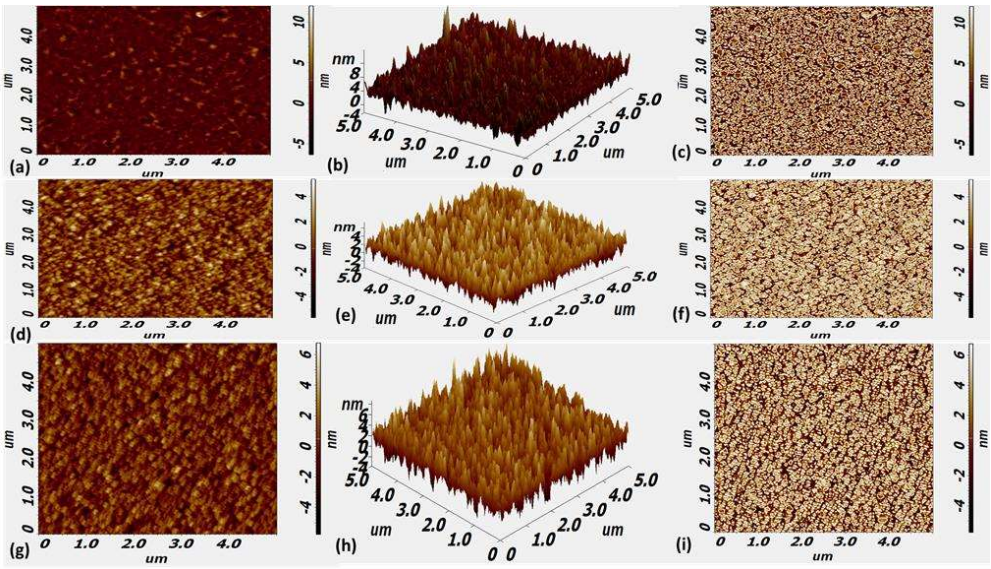

Figure 3.2 2-D AFM image, 3-D AFM image, and Grain analysis image of ((a)-(c)) Pristine PCPDTBT, ((d)-(f)) PCPDTBT/CdS composite, and ((g)- (i)) Photoirradiated PCPDTBT/CdS composite respectively.

Additionally, we have optimized the thickness of the polymer-composite film by varying the composite solution's concentration and composition and temperature of the liquid substrate. Firstly, we observed that decreasing the thickness increases the sensitivity to certain film thicknesses and then starts decreasing. This observed phenomenon is consistent with the published literature [68]. The optimized film thickness of ~20 nm was measured by Filmetrics F20-UV and also verified by AFM.

Table 3.1 AFM parameters of pristine and polymer nanocomposite

Parameters	Pristine PCPDTBT	PCPDTBT/CdS nanocomposite	Photoirradiated PCPDTBT/CdS nanocomposite
RMS roughness (nm)	2	2.3	2.5
Average grain size (nm)	82	79	65
Average grain length (nm)	125	120	99

3.4 Results and discussion

3.4.1. Electrical Characterization

Electrical characterization of the fabricated OFET device was performed using Agilent KEYSIGHT- B1500 semiconductor parameter analyzer, and the performance of the device was assessed with transfer and output/drain characteristics. Some essential transistor parameters, such as charge carrier mobility (μ_P) and threshold voltage (V_{TH}) were taken into consideration from these behavioral curves to assess the electrical parameters of the fabricated OFET device. The output characteristics of the OFET is plotted by varying source- drain voltage (V_{DS} = 0 V to -40 V) for a fixed gate to source voltages (0 to -40 V with a step size of 8). **Figure 3.3**(a) shows the output/drain characteristics plot of the fabricated organic FET. In same manner, the transfer characteristics of the device is plotted by changing the source- drain voltage in fixed steps (0 to -40 V with a step size of 8) while sweeping the gate-source voltage (V_{GS} = 0 V to -40 V) as depicted in **Figure 3.3(b).** The following equation was used to get the drain current (I_{DS}) of the OFET in the saturation regime [76]-

$$I_{DS} = \frac{1}{2}\mu_P C_{OX}\frac{W}{L}(V_{GS} - V_{TH})^2 \; ; \; V_{DS} \geq V_{GS} - V_{TH} \quad \textbf{(3.1)}$$

Where μ_P, C_{OX}, W/L, and V_{TH} represent the mobility, capacitance per unit area of the dielectric layer, aspect ratio (AR) of the channel, and threshold voltage respectively. Threshold voltage and mobility are extracted graphically using the linear fitting of equation, where n and m are the intercept and slope, respectively. The mobility and threshold voltage of the OFET can be obtained by **Equation (3.3). Equation (3.1)** can be rewritten

as:

$$\sqrt{I_{DS}^{sat}} = \sqrt{\frac{1}{2}\mu C_{OX}\frac{W}{L}}\,(V_{GS} - V_{TH}) = \; mV_{GS} - n \tag{3.2}$$

$$\mu = \frac{2L}{WC_{ox}}\,m^2, V_{TH} = \frac{-n}{m} \tag{3.3}$$

The trap charge carrier density of the fabricated device is calculated by-

$$\Delta_{Trap} = \frac{\Delta V_{TH} * \; C_{OX}}{q} \tag{3.4}$$

Table 3.2 demonstrates that the mobility reduces with increasing H_2S gas concentration, while the threshold voltage and trap charge carrier density increase. This phenomenon is evident due to the drain current reduction as the concentration of the exposed H_2S gas increases. The drain current of the fabricated OFET is decreased as a result of the H_2S gas molecules trapping the majority charge carrier (holes) at the sensing surface and depleting the number of charge carriers in the channel.

Table 3.2 OTFT parameters with exposed H_2S gas

H_2S ppm	V_{th} (Volts)	Mobility $*10^{-3}(cm^2/V.\,s)$	Trap density $(*10^{11}/cm^2)$	I_{DS} (µA)	S (%)
0	-4.9	3.41	0	8.3	0
0.1	-6.52	2.42	0.11	5.78	30.4
0.2	-9.1	2.05	1.82	4.27	48.5
0.3	-9.25	1.66	2.78	3.25	60.8
0.5	-9.59	1.47	3.36	2.59	68.8
0.7	-9.76	1.22	3.44	2.13	74.3
0.8	-9.93	1.06	3.54	1.87	77.5
0.9	-9.15	1.01	3.61	1.75	78.9
1	-9.46	0.96	3.81	1.64	80.2

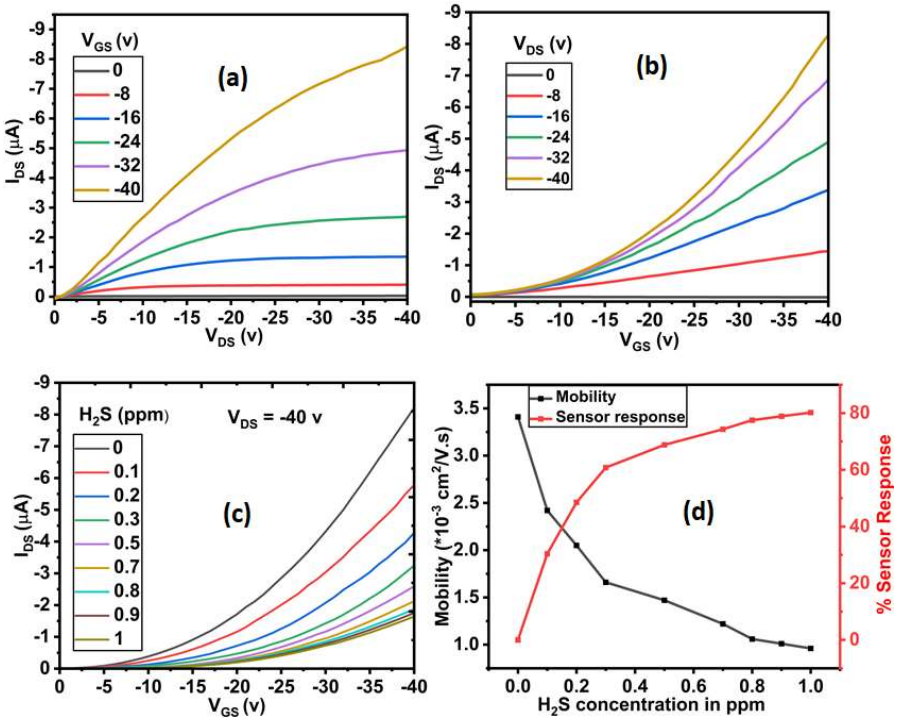

Figure 3.3 (a) Drain characteristics, (b) Transfer characteristics, (c) Drain current variation with H_2S concentration, and (d) Mobility and sensor response variation with H_2S concentration.

3.5 Gas Sensing Parameters

3.5.1. Gas Sensing Response

The response of the fabricated sensor has been calculated using the change in drain current after exposure to H_2S gas for different concentrations. A maximum response of 80.2 % was obtained for a concentration of 1 ppm hydrogen sulfide gas. Sensor response was calculated using the following formula –

$$S\% = \frac{|I_{DS(AIR)} - I_{DS(GAS)}|}{I_{DS(AIR)}} * 100\% \quad \textbf{(3.5)}$$

Drain current variation and sensor response with the increasing concentration of H_2S gas is plotted in **Figure 3.3(c)** and **Figure 3.3(d),** respectively. **Figure 3.4 (a)** demonstrates threshold voltage and trap charge density variation with H_2S concentration.

3.5.2. Selectivity

The OTFT sensor has exhibited maximum response upon exposure to H_2S gas in comparison to other tested gases and demonstrated highly selective behavior towards H_2S

exposure. Selectivity investigation data is presented in **Figure 3.4(b).** Selectivity test has been performed using 1 ppm concentration for H_2S and 10 ppm concentration for other gases.

3.5.3. Stability and Relative Humidity Influence Analysis

To test the stability and robustness of the fabricated sensor at ambient conditions, we have plotted the drain current degradation without exposure to the gas, and sensor response degradation to 1 ppm exposure of H_2S gas for every week continuously up to 8 weeks. The fabricated sensor has shown significant stability over 8 weeks. Drain current degraded up to 10.8% and sensor response up to 9%, over this period of time. Further, we have investigated the effects of RH variation on the sensor performance and concluded that, at lower RH the sensor response is almost stable up to 55% RH. At higher RH conditions, sensor response degrades up to 7.7% for 85% RH level. RH and stability analysis investigation data are presented in **Figure 3.4(c)** and **Figure 3.4(d),** respectively. There is uncertain dependence of gas response on relative humidity. Water molecules help water-soluble analyte gases to adsorb on the sensing surface and enhance the sensor response, whereas hydrogen sulfide is sparingly soluble in water therefore water molecules adsorb onto the active sensing layer and reduce the effective adsorption sites for H_2S adsorption which results in the sensing response reduction at higher humidity levels [94]. A very effective humidity compensation algorithm is proposed in the literature [95], which we will try to incorporate in near future works.

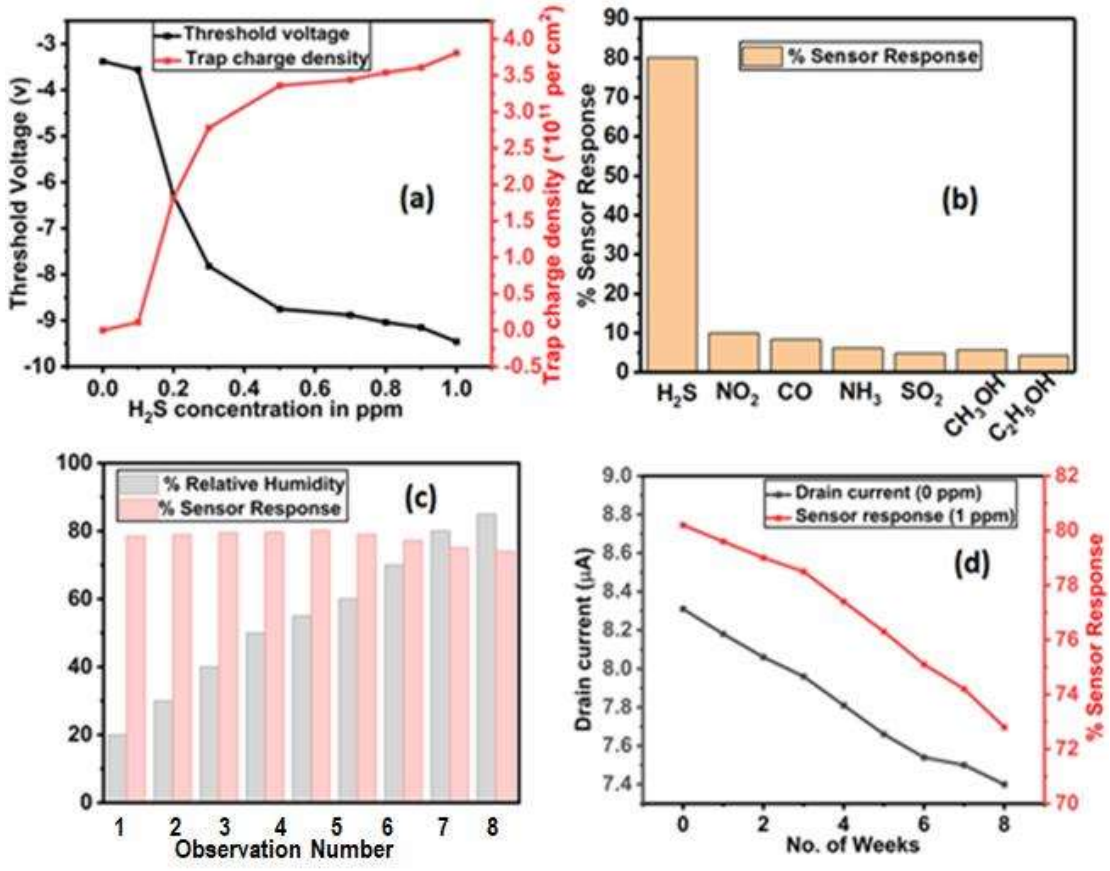

Figure 3.4 (a) Threshold voltage and trap charge density variation with H_2S concentration, (b) Selectivity, (c) Sensor response variation with %RH, and (d) Drain current (without H_2S exposure) and sensor response (with 1ppm H_2S exposure) variation with time.

3.5.4. Repeatability and Transient Analysis

To evaluate the device's repeatability and response-recovery characteristics, we performed the exposure and recovery cycles four times using 1 ppm H_2S gas. The tested device exhibits excellent repeatability, as shown in **Figure 3.5(a),** with almost identical sensor responses to every cycle. We further zoomed in to evaluate the device's response and recovery time (**Figure 3.5(b)**), which were discovered to be ~5 seconds and ~90 seconds, respectively.

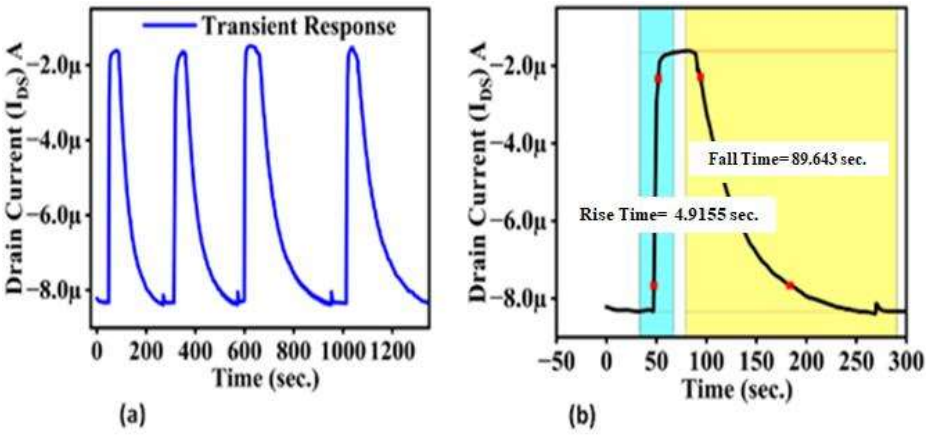

Figure 3.5 (a) Transient analysis at 1 ppm for 4 consecutive cycles (b) Zoomed in image of a transient cycle to show response-recovery time.

3.5.5. gas sensing mechanism

The sensing capabilities of an organic thin film can be affected by a variety of parameters, including the molecular structure of the organic semiconductor, degree of aligned nature of the film, functional groups present in the polymer, film thickness, surface morphology of the organic film, and the organic film's grain boundaries [68][79][80]. As explained in previous sections, all the parameters mentioned above have been improved significantly and contribute towards enhanced sensing performance. Although CdS is a n-type semiconductor with electrons as majority carriers but the nanocomposite only contains 5% (w/v) amount of CdS. Therefore, overall behavior of the nanocomposite is of p-type. Furthermore, the gas sensing mechanism can be described in two steps; charge injection (adsorption or physisorption) and charge transport. BTD functional groups could be employed as the units of electron acceptors for semiconducting materials due to their significant electron-withdrawing ability [81]. Possible adsorption mechanism as follows: BTD is a very strong e^- accepting unit because it contains two electron-withdrawing imine nitrogen atoms (C=N). Also, nitrogen has much higher electronegativity than sulfur. Therefore, sulfur will be electron deficient and develop a partial negative charge. Further, the

lone pairs of hydrogen sulfide gas will get attached to the sulfur atom of BTD functional group via strong van der waals force. In case of CPDT, although it is an electron donor group but due to slightly more electronegativity of carbon atom than sulfur, the sulfur atom will develop a much lower partial negative charge compared to the sulfur of BTD group. Therefore, the lone pairs of hydrogen sulfide gas will get attached to the sulfur atom of CPDT functional group via weak van der waals force. These adsorbed/injected electrons will trap the holes of the sensing film. As a result, carrier density and drain current are reduced and this phenomenon is called 'charge trapping' in the sensing film. I_{DS} tends to stabilize once the number of H_2S molecules adsorbed on the sensing surface reach at saturation due to unavailability of vacant adsorption sites. The adsorbed H_2S molecules are gradually desorbed when the sensing material is exposed to air again or the gas ambiance removed, thus increasing the I_{DS}. After desorption of H_2S molecules from the sensing film, I_{DS} slowly recovers back towards the baseline level. Possibly, desorption occurs first at weak van der Waals force adsorption sites followed by strong adsorption sites, resulting in higher recovery time compared to response time. Now, the possible charge transport mechanism as follows: Firstly, we will explain the charge transport mechanism in pristine PCPDTBT chain, further we will explain the charge transport mechanism in the composite film. Charge transport along the PCPDTBT film take place via the conductive paths formed by the mutually overlapping π orbits of the PCPDTBT rings. Charge transport process can be described with the help of intrachain and interchain transport. Polymer film can be represented as the matrix of connected individual polymer chains. Charge transport occurs dominantly due to intrachain process because of the enhanced molecular ordering of the sensing film. Interchain transport occur in the regions where the polymer chains are disordered [75]. We can see the intrachain and interchain transport mechanism in the **Figure 3.6**. Straight tie chain intercrystallite connections

(high order alkyl side chains to connect two polymer chains, also called interchain coupling) are expected to promote the high mobility over the extended backbone of polymer chains from crystallite to crystallite. In case of, presence of disordered regions and amorphous phases surrounding the crystallite domains, high amount of interchain packing supports conjugated polymers for charge carrier localization via interchain transport process [75]. Now, let's discuss the charge transport mechanism of composite film. Doping is the chemical modification of a polymer's structure to generate charge carriers in the polymer chain by charge exchange with the dopant species. The net distribution of the positive charge also gets influenced by the introduction of the dopant CdS on the polymer backbone. Carrier delocalization occurs along the chain of the polymer due to the attraction force exerted by the nuclei of one repeat unit to the electron of the other repeat unit, which results in carrier transport via intra and interchain transport process [96]. This type of dopants is considered as primary dopants, which change the electronic, structural, magnetic, and optical properties of the polymer, along with a change in conductivity. A secondary dopant (H_2S analyte in this case) is considered as a substance that upon exposure to a primary-doped polymer, alters the inherent properties. In PCPDTBT/CdS hybrid nanocomposites, the modification of hole transport characteristics, including an increase in trap density and characteristic trap energy as well as an improvement in hole mobility, may be explained in terms of charge transfer-type interactions between the PCPDTBT host and CdS guest. Nevertheless, the increase in charge carrier mobility suggests that the primary mode of interaction between the host and guest may be the development of charge transfer complexes (CTCs). The band gap of the host PCPDTBT may experience favorable energy states produced by guest CdS NPs. These favorable energy states within the band gap are known as traps, and as illustrated in **Figure 3.7(a),** which further results in increase of trap density and characteristic trap energy.

Through the trap states, CdS NPs provide extra decaying pathways for the excited carriers. As a result, the CdS NPs aid the charge carriers that previously had to cross from one polymer chain to another in order to transport across the PCPDTBT film, increasing charge carrier mobility. Thus, compared to pristine polymer thin films, charge carriers may flow more readily in PCPDTBT/CdS composite thin films. As a result, the introduction of CdS NPs increases the hole mobility in PCPDTBT.

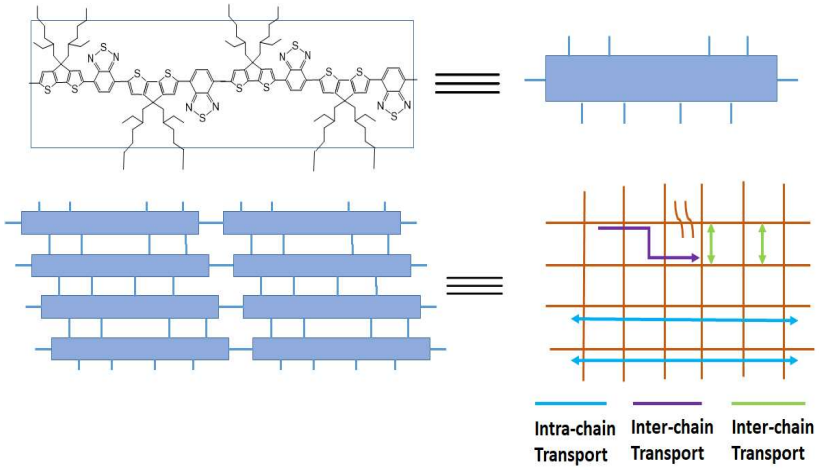

Figure 3.6 Charge carrier transport in polymer backbone.

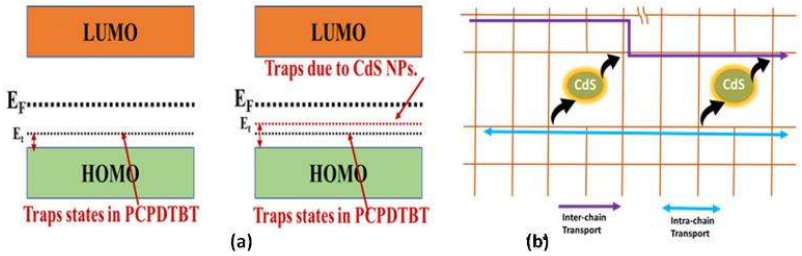

Figure 3.7 (a) Distribution of traps energy states with-in the band gap of PCPDTBT and PCPDTBT/CdS (b) Charge carrier transport in polymer nanocomposite matrix.

The composite sensing film can be interpreted as a matrix that assist on carrier transport with the help of redox centers (**Figure 3.7(b)).** The secondary dopant/analyte being sensed forms a charge transfer complex between the sensing film and the analyte, which further modifies the surface morphology and electrical properties of the sensing film, as explained earlier. Since the interaction force (Van der Waals) involved between the

secondary dopant and the composite film is low, the modification of the electronic properties of the sensing film is reversible, which results in complete recovery of the fabricated device and displays an excellent repeatable and reversible nature of the fabricated gas sensor.

3.6 Conclusion

As stated in the abstract of this chapter, the aim of this work was to enhance the shortcomings of previous chapter such as poor recovery characteristics, environmental degradation, significant reliance on relative humidity variation, less mobility, and a possibility to further enhance the sensing response. Photoirradiated PCPDTBT/CdS nanocomposite film exhibits a maximum charge carrier mobility of ~$3.4*10^{-3}$ $cm^2/V.$ s, which is many folds higher than that obtained in previous chapter. Additionally, the photoirradiated-SVA annealed PCPDTBT/CdS composite sensor achieves significantly enhanced response of ~81% to 1 ppm exposure of H_2S gas, compared to obtained in previous chapter (~71%). Additionally, excellent response-recovery behaviour (e.g., ~5 s and ~ 90 s, respectively), good ambient stability, and stability against relative humidity variations are also observed. In summary, a facile method that enhanced the interfacial charge interactions and charge transport between PCPDTBT and CdS components in PCPDTBT/CdS composites, employing a simple photoirradiation methodology has been reported in present work. This method in conjunction with FTM deposition and solvent vapor annealing improved the molecular ordering of the PCPDTBT matrix, resulting in higher charge carrier mobility in the final PCPDTBT/CdS nanocomposite. The photoirradiated PCPDTBT/CdS composite film was used to develop an OFET gas sensor with exceptional sensitivity to hydrogen sulphide gas. According to investigations, a charge transfer complex (CTC) is formed between the host PCPDTBT and the guest CdS nanoparticles (NPs). The introduction of CdS NPs to the polymer matrix increases traps density and, as

a result, characteristics trap energy, which may be attributed to the extra favorable energy states generated by CdS nanoparticles within the energy band gap of PCPDTBT. Furthermore, the transfer of charge carriers is aided by these favorable trap states to move faster, resulting in increased mobility of holes in the nanocomposite system. Based on these findings, it is evident that the PCPDTBT/CdS hybrid system has outstanding electrical and gas sensing properties and can be used in highly efficient hydrogen sulphide gas sensors. These OFET sensors also demonstrated exceptional response/recovery characteristics, outstanding selectivity, and good ambient stability.